Linnæus University
Sweden

Master Thesis in Mechanical Engineering

Experimental acceleration Measurements and Finite Elements Modeling

Author: Ibrahim Alnimairi, Salim Arrabi
Supervisor: Lars Håkansson, Tatiana Smirnova
Examinar: Lars Håkansson
Linnaeus University, Faculty of Technology,
Department of Mechanical Engineering

Abstract

Heavy crushing machines under their production shifts, creates various levels of vibration, noise and dynamic forces which can be transferred to other parts of the industrial unit. Such kind of factors applies continuous forces on machine parts which can cause gradual fatigue, creep and eventually failure of machine.

In this thesis work we are studying Jaw crusher machine from Sandvik company, since the company has a high focus on safety and quality, this thesis is aiming to estimate the dynamic foundation loads that are transmitted to substructure of the jaw crusher.

The thesis is based on estimating power spectral density transmissibility matrix-single value decomposition (PSDTM-SVD), between jaw crusher foot (CRF), side wall (SW) and substructure (SS) in x, y, z positions to identify model parameters including damped eigenfrequencies and mode shapes.

This research has concluded that it is possible to estimate the transmitted load force by finding the relation between displacement transmissibility and force transmissibility by employing (PSDTM-SVD) method. In fact (PSDTM-SVD) is a sufficient method to estimate the damped eigenfrequencies and mode shapes during operation.

Nevertheless, it is majorly important to have good coherence between measured data, in this case data that have been conducted in Y direction had a good coherence of 0.9.

Linnæus University
Sweden

Acknowledgement

We would like to thank our thesis supervisor prof. Lars Håkansson. The door to office was always open whenever we had troubles during the preparation of this thesis work.

He consistently allowed this thesis to come out to the light by assisting and steering with related and necessary knowledge for this research work.

I would also like to thank Sandvik AB company for suppling us with data and explaining the problem statement of this thesis.

I would also like to acknowledge Mr. Lech Muszyński and Mr. per Lindström (Faculty of mechanical engineering) as a second readers and reviewers of this thesis, and we are gratefully appreciating their very valuable comments and guidance during this thesis work.

Finally, we must express our very profound gratitude to our parents who provided us with unconditional support and continuous encouragement throughout the time of writing and researching. This accomplishment would have never been possible without their love and support.

Table of contents

1. Introduction

Gravel is one of the most useful components in construction, railway building, roads, and other industrial fields [1]. Moreover, In Europe and North America gravels are widely used during the winter seasons to prevent slipping on the highway roads, in addition to that gravels play a substantial role in reinforced concrete [1].

There are different types of crushers that are used in gravel production, for example, Jaw crusher, Gyratory crusher, cone crusher, impact crusher and many more [1]. In this project jaw crushers are considered. In Fig. 1 a jaw crusher is shown.

Jaw crushers are used as a first step of material size reduction both in construction (producing gravel) and in mining application, when the purpose is to reduce size of the particles by different types of crushing down to millimeters and even to micrometers, so it is possible to extract metal ore from the resulting product) [1].

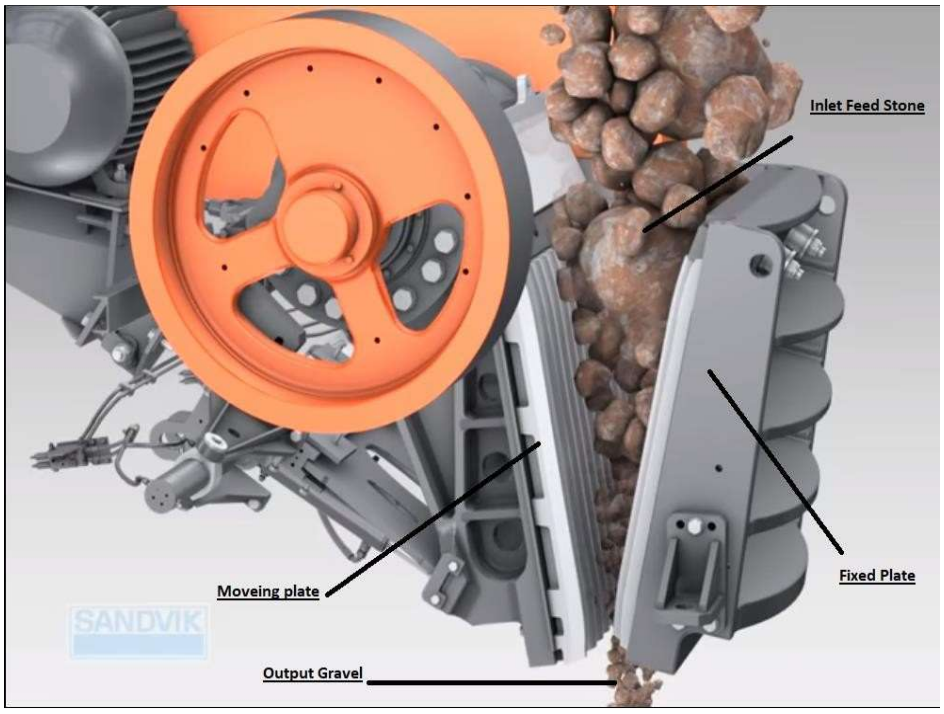

Figure 1: Jaw Crusher [14]

1.1 Background and problem description

1.1.1 Literature Review

The jaw crusher is versatile, and it can be used to crush rocks, whose hardness may range from medium-hard to extremely hard which mean that the rock could be tough and need high toad to crush or could be soft that need low load to crush, as well as different kinds of ore, building rubble. They are widely used in a variety of demolition, extraction, reclamation, and recycling industries, but particularly, in the mining and construction sectors [4].

Practically, an insight look into the core of the jaw crusher might be very helpful to gain more understanding of its crushing mechanism and how the rocks are crushed [5].

Mainly Jaw crushers consists of two hard metallic plates, the jaws, that have a high hardness index, which is sufficient to handle the hardness of the crushed materials [5].

The two metallic plates are mounted with an inclination towards each other that forms a vertical V shape where the inlet area is wider than outlet area. One of the jaw plates is fixed while other plate is movable, and the controlled motion of this plate induce the crunching of the rock [5].

When a Jaw crusher operates its inlet, area is fed with rock material and the movable plate will apply a cyclic load on the material and compress the material against the fixed plate, thus, causing a high compressive load. Under the influence of gravity, the rock pieces will pass vertically trough a Jaw crusher and the material will be successively crushed to become mall enough to pass through the narrower output of V shaped space between the jaws [5].

The jaw crusher is a portable machine, which means that it may be mounted on trucks or trailers to make it mobile and thus it may easily be moved between different projects sites. Moreover, a jaw crusher is also relatively easy to disassemble and to relocate to different work environments [6].

This allows a jaw crusher to be used and to operate on the surface as well as underground in mining projects. In fact, simplicity in structure and in operation as well as their reliability and ease of maintenance are some of the advantages of jaw crushers. One more advantage is the high capacity of a jaw crusher compared to the other types of crusher such as cone crusher, gyratory crusher and the different designs of impact crushers [7].

There are two types that are mainly used in the field of crushing, single toggle, and double toggle jaw crusher. The last one originally was designed by Elo Whitney Blake in USA in 1857 [8].

The most interesting advantage of the double toggle is the swing jaw plate motion, it is being designed to apply a concentrated compressive force on the crushed material, this actually minimizes the wear of crushing surfaces of the jaws, that is also make double toggle jaw crushed the very effective to crush a highly abrasive and very hard materials. Indeed, even in these days Blakes designs of the double toggle jaw crusher is still in use in mines and quarries probably with some minor improvements [8].

1.1.2 Description of Jaw crusher installation

A jaw crusher installation consists of main three parts: (i) crusher (ii) Attachment (iii) Substructure

Where the crusher is responsible for crashing the stone, Attachment is the way of connection between crasher and substructure, while sub structure is the base that supports the crusher, see Fig. 2.

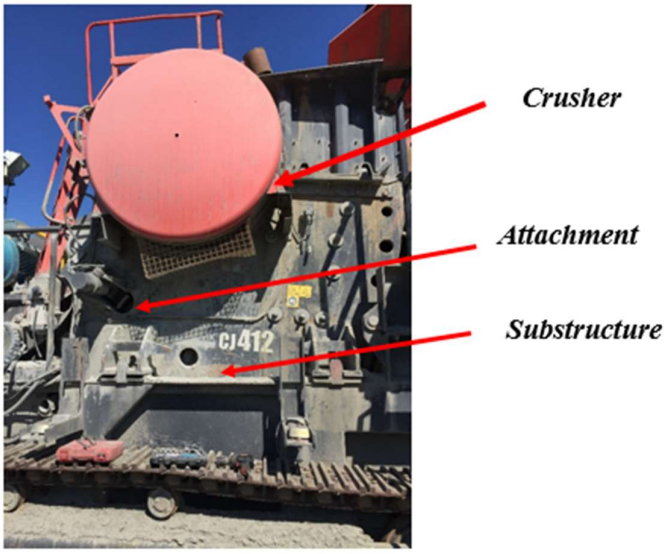

Figure 2: An example of the crusher attachment to one of the several types of substructures [14]

1.1.3 Problem description

Since the crushing process applies broad band excitation both to the crusher and to the substructure it is attached to, the broad band excitation can potentially trigger the natural mode shapes of the "crusher -substructure" system. It is of interest to identify the magnitude of loads transmitted by the crusher in operation to the substructure. This is necessary to design robust and reliable sub-structures.

1.2 Aim and purpose

The aim of this study is to find a new approach to predict foundation loads due to the crushing process.

1.2.1 Motivation

Identifying a method to estimate loads, originating from the stone crushing process, transmitted to the Jaw crusher substructure, will contribute to design of robust and reliable sub-structures for crusher installation.

1.3 Hypothesis and limitations

By using measured acceleration data, one should be able to estimate the excitation load applied on the crusher and on the substructure, which proportionally have a direct effect on the jaw crusher foundations load.

1.3.1 Limitations

This study will be performed only on Sandvik jaw crusher model number (CJ 412), it is worthy to mention that our measured data has been collected from this model.

1.4 Reliability, validity, and objectivity

The measurements been collected in term to accomplish this research, has been done by SANDVIK company, an accelerometer measuring instrument been used to collect this data.

Acceleration Time Series measured with sampling frequency Fs=2000 Hz, accelerometers been attached to three different parts of Jaw crusher, each time 2 accelerometer are attached to 2 part of the 3 parts of the Crusher each time then the test take place. Which mean that each test we have 2 accelerometers attached to 2 parts for example

Case 1 one accelerometer is attached to SW (Side wall of the crusher) and the other one is attached to SS (substructure) then in case 2 one is attached to CRF (Crusher foot) while the second is attached to SS (substructure) and so on.

The data will be more accurate by measuring in this way since we collect data from two different instruments simultaneously.

CRF (Crusher foot)

SW (Side wall of the crusher)

SS (substructure)

1.5 Authors' contribution

Salim A. and Ibrahim. A has contributed to half basis on this research by combination work and literature study regarding this thesis.

2. Materials and Methods

2.1 Experimental Setup

Vibration experiments were carried out on a Sandvik Jaw Crusher, model CJ412 and this crusher consist of 3 main parts which are: -CRF (Crusher foot); - SW (Side wall of the crusher); - SS (substructure), see figure 3.

2.1.1 Measurement Equipment and setup:

In the measurements 2 triaxial accelerometers were used and four different measurements were carried out. In each measurement the accelerometers were attached to different unique positions on the jaw cruncher. For instance, in one measurement one accelerometer was attached on the Crusher foot (CRF) and the other accelerometer was attached on the one on the side wall of the crusher (SW), see Fig. 3. In the measurements the sampling frequency used for the data acquisition was F_s=2000 Hz. Each of the accelerometers measure vibration in three orthogonal directions: The x-direction; the acceleration in the crusher's longitudinal direction, the y-direction; the acceleration in the crusher's vertical direction and the z-direction; the acceleration in the crusher's transverse/lateral direction.

The measurement equipment consisted of:

- 2 Accelerometers, dynamic range +-16g, frequency range 1500 Hz in x- and y-directions, and 550 Hz in z-direction ‘.
- DEWESOFT data acquisition system.
- MATLAB.
- PC computer.

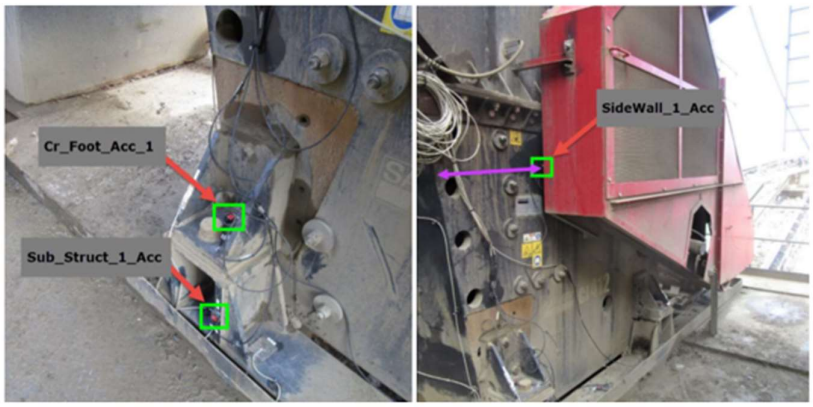

Figure 3: An example of the accelerometer attachment on the Jaw crusher.

2.2 Structural Dynamics:

2.2.1 Equation of motion for Multi-degree-of-freedom (MDOF) System in the Frequency Domain:

For simplicity, the multiple-degrees-of-freedom system is represented in terms of a two-degrees-of-freedom system and in Fig. 4 a two-degrees-of-freedom system is illustrated.

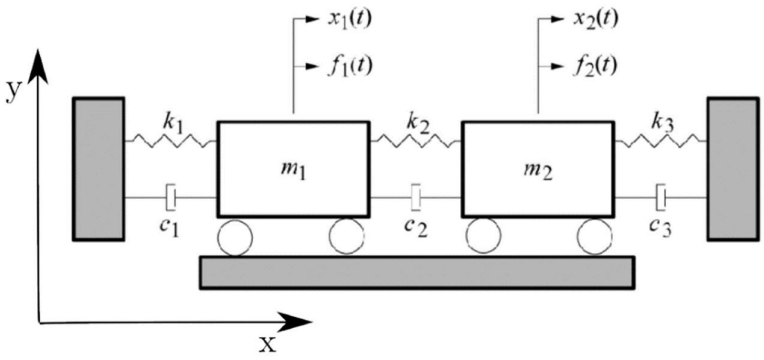

Figure 4: A two-degrees-of-freedom system [12]

Where m1 is the mass of mass one [kg], m2 is the mass of mass two [kg], c1 is the damping coefficient of damper one [N/m/s], c2 is the damping coefficient of damper two [N/m/s],k1 is the stiffness of spring one [N/m], k2 is the stiffness of spring two [N/m], k3 is the stiffness of spring tree [N/m], $f_1(t)$ input force acting on mass one (N), $f_2(t)$ input force acting on mass two (N), $X_1(t)$ is the displacement output of mass one [m], $X_2(t)$ is the displacement output of mass two [m].The equations for the two-degrees-of-freedom system may with the aid of newton's second law be expressed as: [12]

$$m_1 \frac{\partial x_1(t)^2}{\partial t^2} + (c_1 + c_2) \frac{\partial x_1(t)}{\partial t} - c_2(t) \frac{\partial x_2(t)}{\partial t} + (k_1 + k_2)\, x_1(t) - k_2(t) x_2(t) = f_1(t) \quad (1)$$

$$m_2 \frac{\partial x_2(t)^2}{\partial t^2} + (c_2 + c_3) \frac{\partial x_2(t)}{\partial t} - c_2(t) \frac{\partial x_1(t)}{\partial t} + (k_2 + k_3)\, x_2(t) - k_2(t) x_1(t) = f_2(t) \quad (2)$$

Rewriting the equation 1 and 2 in terms of vectors and matrices results in [12]

$$\begin{bmatrix} m_1 & 0 \\ 0 & m_2 \end{bmatrix} \begin{Bmatrix} \frac{\partial x_1(t)^2}{\partial t^2} \\ \frac{\partial x_2(t)^2}{\partial t^2} \end{Bmatrix} + \begin{bmatrix} C_1 + C_2 & -C_2 \\ -C_2 & C_2 + C_3 \end{bmatrix} \begin{Bmatrix} \frac{\partial x_1(t)}{\partial t} \\ \frac{\partial x_2(t)}{\partial t} \end{Bmatrix} + \begin{bmatrix} K_1 + K_2 & -K_2 \\ -K_2 & K_2 + K_3 \end{bmatrix} \begin{Bmatrix} x(t) \\ x(t) \end{Bmatrix} = \begin{Bmatrix} f_1(t) \\ f_2(t) \end{Bmatrix} \quad (3)$$

In general form the equations of motion for the two-degrees-of-freedom system may be written as:

$$[M]\{\ddot{x}(t)\} + [C]\{\dot{x}(t)\} + [K]\{x(t)\} = \{f(t)\} \quad (4)$$

Where [M] is the mass matrix (kg), [C] is the damping matrix [Ns/m], [K] is the stiffness matrix [N/m], $\{x(t)\}$ is the displacement vector [m], $\{f(t)\}$ is the force vector [N]. The equations of motion in the frequency domain for a two-degrees-of-freedom system may be expressed as

$$-\omega^2[M]\{X(f)\} + j\omega[C]\{X(f)\} + [K]\{X(f)\} = \{F(f)\} \quad (5)$$

$$\Leftrightarrow$$

$$(-\omega^2[M] + j\omega[C] + [K])\{X(f)\} = \{F(f)\} \quad (6)$$

Here ω=2πf is the angular frequency [rad/s], f is the frequency [Hz], $\{X(f)\}$ is the Fourier transform of the displacement vector [ms] and $\{F(f)\}$ is the Fourier transform of the force vector [Ns]. Thus, displacement vector in the frequency domain is given by

$$\{X(f)\} = (-\omega^2[M] + j\omega[C] + [K])^{-1}\{F(f)\}$$

$$\Leftrightarrow$$

$$\{X(f)\} = [H(f)]\{F(f)\} \quad (7)$$

Where [H(f)] is the frequency response function matrix. In the case of a two-degrees-of-freedom system, the frequency response function matrix is given by:

$$[H(f)] = \begin{bmatrix} H_{11}(f) & H_{12}(f) \\ H_{21}(f) & H_{22}(f) \end{bmatrix} \quad (8)$$

Where $H_{mn}(f)$ is the frequency response function between the response coordinate m and the force coordinate n, $m, n \in \{1, 2\}$. The frequency response matrix may be expanded as

$$[H(f)] = \sum_{m=1}^{2} \left(\frac{1}{a_m} \frac{\{\Psi\}_m \{\Psi\}_m^T}{j2\pi f - \left(-\omega_m \zeta_m + j\omega_m \sqrt{1-\zeta_m^2}\right)} + \frac{1}{a_m^*} \frac{\{\Psi\}_m^* \{\Psi\}_m^H}{j2\pi f - \left(-\omega_m \zeta_m - j\omega_m \sqrt{1-\zeta_m^2}\right)} \right) \quad (9)$$

Where $\{\Psi\}_m$ is the mode shape vector for mode m, ω_m is the un-damped angular resonance frequency for mode m, ζ_m is the relative damping coefficient for mode m and a_m is the modal A coefficient for mode m. Furthermore, * denotes complex conjugation and $\{\bullet\}^H$ is the Hermitian transpose of the vector.

2.2.2 Transmissibility for multiple - degrees of freedom (MDOF) systems

There are two 2 types of transmissibility that are taken in considiration here, i) Displacement transmissibility and ii) Force transmissibility.

Infact the expression of force and displacement tranmissibility are idintical in terms vibration isolation SDOF problems, while they are not in case of MDOF problems [13].

Y.E. Lage et. al. reports how force and displacement transmissibilities for MDOF systems may be related and corresponding required conditions [13].

In Fig. 5 a single-degree-of-freedom system is illustrated.

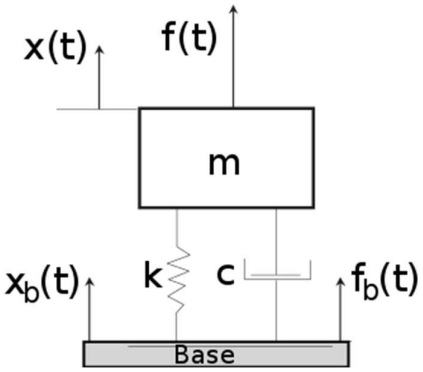

Figure 5: A single-degree-of-freedom system

Based on the SDOF system in Fig. 5 the transmissibility concept will be introduced. The displacement transmissibility $T^d(f)$ between the response of the mass x(f) and the motion of the base $x_b(f)$ is defined as [13]:

$$T^d(f) = \frac{X(f)}{X_b(f)} \qquad (10)$$

Where X(f) is the Fourier transform of the response of the mass and X_b(f) is the Fourier transform of the base motion. In the case of displacement transmissibility, it is assumed that there is no external force acting on the mass m, f(t)=0, The equation of motion for the case of base motion is given by:

$$m\frac{d^2x(t)}{dt^2} = -c\frac{dx(t)}{dt} + c\frac{dx_b(t)}{dt} - \mathrm{kx(t)} + \mathrm{k}x_b(t)$$

$$\Leftrightarrow$$

$$m\frac{d^2x(t)}{dt^2} + c\frac{dx(t)}{dt} + \mathrm{kx(t)} = c\frac{dx_b(t)}{dt} + \mathrm{k}x_b(t) \qquad (11)$$

The Fourier transform of this expression yields:

$$(-\omega^2 m + j\omega c + \mathrm{k})\mathrm{X(f)} = (j\omega + \mathrm{k})X_b(f)$$

$$\Leftrightarrow$$

$$T^d(f) = \frac{X(f)}{X_b(f)} = \frac{(j\omega + \mathrm{k})}{(-\omega^2 m + j\omega c + \mathrm{k})} \qquad (12)$$

No we concider the case of force transmissibility T^f(f) between the force acing on the base f_b(t) and the force acting on the mass f(t), is defined as [13]

$$T^f(f) = \frac{F_b(f)}{F(f)} \qquad (13)$$

Where F(f) is the Fourier transform of the force acing the mass and F_b(f) is the Fourier transform of the force acing on the base. For the case of force transmissibility it is assumed a rigide base (x_b(t)=0). The equations of motion may now be written as:

$$\begin{cases} m\frac{d^2x(t)}{dt^2} + c\frac{dx(t)}{dt} + \mathrm{kx(t)} = f(t) \\ c\frac{dx(t)}{dt} + \mathrm{k}x(t) = f_b(t) \end{cases} \qquad (14)$$

The Fourier transform of these equations yields:

$$\begin{cases}(-\omega^2 m + j\omega c + \mathrm{k})\mathrm{X(f)} = F(f) \\ (j\omega + \mathrm{k})X(f) = F_b(F)\end{cases}$$

$$\Leftrightarrow$$

$$T^f(f) = \frac{F_b(f)}{F(f)} = \frac{(j\omega + \mathrm{k})}{(-\omega^2 m + j\omega c + \mathrm{k})} \qquad (15)$$

Thus, if the force transmissibility for a SDOF system is Known then the displacement transmissibility for the SDOF is also known and vice versa is also true [A.Brandt]. Now the discussion is extended to the case of multiple-degrees-of-freedom (MDOF) system. To address displacement transmissibility and force transmissibility for MDOF systems two sets of coordinates are defined, the K set and the U set, see Fig. 6. In Fig. 6 a) the elastic body with two rigid supports is illustrated and b) the corresponding free elastic body is illustrated.

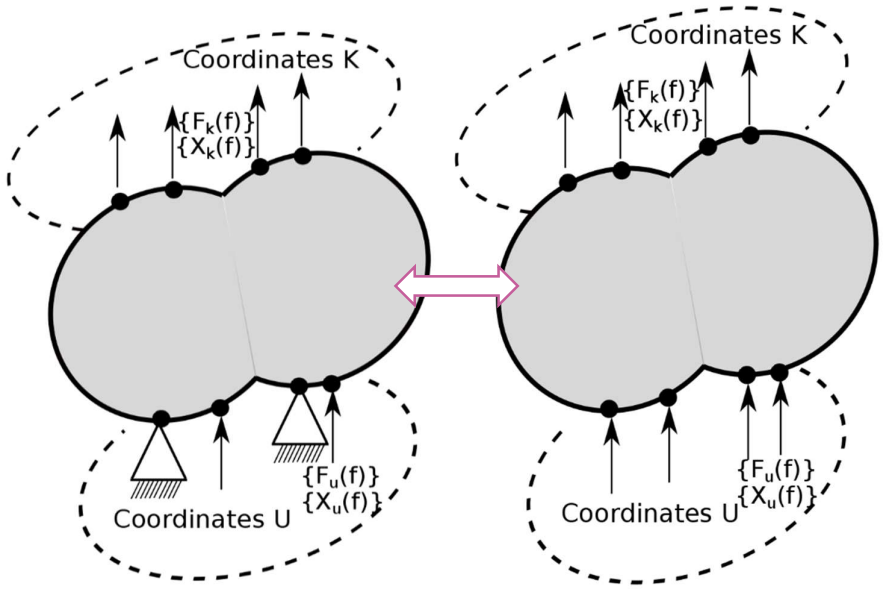

a) b)

Figure 6: a) elastic body with two rigid supports and b) the corresponding free elastic body. Here two sets of coordinates are defined; the K set and the U set [13].

In the K set we may have external forces acting on the body and their Fourier transforms constitute the components of the force vector $\{F_k(f)\}$ and the Fourier transforms of the displacement responses constitute the components of the displacement vector $\{X_k(f)\}$. Furthermore, in the U set we may have both external forces and reaction forces acting on the body and their Fourier

transforms constitute the components of the force vector $\{F_u(f)\}$ and the Fourier transforms of the displacement responses constitute the components of the displacement vector $\{Xu(f)\}$. The displacement responses of the elastic body is related to the forces acting on it as:

$$\begin{Bmatrix}\{X_k(f)\}\\ \{X_u(f)\}\end{Bmatrix} = \begin{bmatrix}[H_{kk}(f)] & [H_{ku}(f)]\\ [H_{uk}(f)] & [H_{uu}(f)]\end{bmatrix}\begin{Bmatrix}\{F_k(f)\}\\ \{F_u(f)\}\end{Bmatrix} \quad (16)$$

Where $[H_{kk}(f)]$ is the frequency response function matrix between the forces and responses at the coordinates in the K set and $[H_{ku}(f)]$ is the frequency response function matrix between the forces at the coordinates in the U set and responses at the coordinates in the K set. Furthermore, $[H_{uk}(f)]$ is the frequency response function matrix between the forces at the coordinates in the K set and responses at the coordinates in the U set and $[H_{uu}(f)]$ is the frequency response function matrix between the forces and responses at the coordinates in the U set. Now it is assumed that the only forces acting on the elastic body in the U set are the reaction forces imposed by the supports. It is also assumed that the totally supports constraint the displacement responses at the coordinates the body is supported, rigid supports. This yields that [13]:

$$\{X_u(f)\} = [H_{uk}(f)]\{F_k(f)\} + [H_{uu}(f)]\{F_u(f)\} = 0$$

$$\Leftrightarrow$$

$$\{F_u(f)\} = -[H_{uu}(f)]^{-1}[H_{uk}(f)]\{F_k(f)\} \quad (17)$$

Thus, the force transmissibility between coordinates in the U set and the K set is given by [13]:

$$\left[T_{uk}^{f}(f)\right] = -[H_{uu}(f)]^{-1}[H_{uk}(f)] \quad (18)$$

Furthermore, the force at the coordinates in the K set and in the U set are related as [13]

$$\{F_k(f)\} = [T_{uk}^{f}(f)]^{+}\{F_u(f)\} \quad (19)$$

Where $[\bullet]^{+}$ is the pseudo-inverse of a matrix $[\bullet]$ and the pseudo-inverse of $[T_{uk}^{f}(f)]$ it is given by:

$$[T_{uk}^{f}(f)]^{+} = -[H_{uk}(f)]^{+}\,[H_{uu}(f)] \quad (20)$$

Here the number of coordinates in U ≥ the number of coordinates in K. Now displacement transmissibility is considered, and it is assumed that the only forces acting on the elastic body are in the U set. It is also assumed that the

totally supports constraint the displacement responses at the coordinates the body is supported, rigid supports. This yields that [13]:

$$\{X_u(f)\} = [H_{uu}(f)]\{F_u(f)\} \quad (21)$$

and

$$\{X_k(f)\} = [H_{ku}(f)]\{F_u(f)\} \quad (22)$$

With the aid of these expressions, a relation between the displacement responses of the coordinates in the K set and the coordinates in the U set may be written as:

$$\{X_u(f)\} = [H_{uu}(f)][H_{ku}(f)]^{+}\{X_k(f)\} \quad (23)$$

Thus, the displacement transmissibility matrix in this case may be written as:

$$\left[T_{uk}^{d}(f)\right] = [H_{uu}(f)][H_{ku}(f)]^{+} \quad (24)$$

Furthermore, the pseudo inverse of this expression is given by

$$\left[T_{uk}^{d}(f)\right]^{+} = [H_{ku}(f)][H_{uu}(f)]^{-1} \quad (25)$$

Now it may be observed that:

$$-\left(\left[T_{uk}^{d}(f)\right]^{+}\right)^{T} = -[H_{uu}(f)]^{-1}[H_{uk}(f)] \quad (26)$$

Hence, a relation between force transmissibility and the displacement transmissibility for the coordinates in the K set and the coordinates in the U if the number of coordinates in U ≥ the number of coordinates in K is given by [13]:

$$\left[T_{uk}^{f}(f)\right] = -\left(\left[T_{uk}^{d}(f)\right]^{+}\right)^{T} \quad (27)$$

If the number of coordinates in K ≥ the number of coordinates in U the displacement transmissibility for the coordinates in the K set and the coordinates in the U in terms of force transmissibility may be expressed as [13]:

$$\left[T_{uk}^{d}(f)\right] = -\left(\left[T_{uk}^{f}(f)\right]^{T}\right)^{+} \quad (28)$$

2.3 Spectral Density

In reality, measured vibration signals usually display random properties and to produce transmissibility functions for a structure based on such signals it suggests a statistical approach. A suitable approach may e.g., be obtained with the aid of the statistical concepts power spectral density and cross-power spectral density [16].

2.3.1 Power Spectral Density (PSD):

For random signals x(t) that at least may be considered as weakly stationary the power spectral density is defined as the Fourier transform of the signals auto-correlation function $r_{xx}(\tau)$ which is defined as[16]:

$$r_{xx}(\tau) = E[x(t)x(t-\tau)] \qquad (29)$$

Where E [•] denotes the expectation. Thus, the power spectral density for the random signals x(t) is given by [16]:

$$P_{xx}^{PSD}(f) = \int_{-\infty}^{\infty} r_{xx}(\tau) e^{-j\,2\,\pi\,f\,\tau} d\tau \qquad (30)$$

Here, f is frequency in Hz. The power spectral density provides the continuous power distribution in the frequency domain for a random signal that at least may be considered as weakly stationary [17]. For measured vibration, such signals are generally analysed in the digital domain based on a sampled version of the vibration signal x(n), n is discrete time. To estimate power spectral density based on a sampled signal the Welch power spectral density estimator may be used and it is given by [17]:

$$\hat{P}_{xx}^{PSD}(f_k) = \frac{1}{F_s L \sum_{n=0}^{N-1}(w(n))^2} \sum_{l=1}^{L} \left| \sum_{n=0}^{N-1} x_l(n) w(n) e^{-j2\pi n \frac{k}{N}} \right|^2, \quad (31)$$

$0 \le k \le N/2\text{-}1, \; f_k = \frac{k}{N} F_s$

Where N is the length of the periodogram, L is the number of periodograms, F_s is the sampling frequency.

2.3.2 Cross Power Spectral Density (CPSD):

The cross-power spectral density (CPSD) between any two weakly stationary signals x (t) and y (t), is given by

$$P_{yx}^{PSD}(f) = \int_{-\infty}^{\infty} r_{yx}(\tau) e^{-j\,2\,\pi\,f\tau} d\tau \qquad (32)$$

Where $r_{yx}(\tau)$ is the cross-correlation function between the signals x (t) and y (t) . The cross-power spectral density may also be estimated for sampled signals x(n) and y(n) with the aid of the Welch power spectral density estimator, according to [16,17]:

$$\hat{P}_{yx}^{PSD}(f_k) = \frac{1}{F_s L \sum_{n=0}^{N-1}(w(n))^2} \sum_{l=1}^{L} \left(\sum_{n=0}^{N-1} y_l(n) w(n) e^{-j2\pi n \frac{k}{N}} \right) \left(\sum_{n=0}^{N-1} x_l(n) w(n) e^{-j2\pi n \frac{k}{N}} \right)^{*} \qquad (33)$$

Where (•)* denotes complex conjugation.

2.4 Frequency response function (FRF) and Coherence:

2.4.1 Frequency Response Function (FRF):

For a single-input-single-output system (SISO system) with one input signal x (t) and one output signal y(t) e.g., a single-degrees-of freedom (SDOF) system its frequency response function may be estimated as [16]

$$\hat{H}_{yx}(f_k) = \frac{\hat{P}_{yx}^{PSD}(f_k)}{\hat{P}_{xx}^{PSD}(f_k)} \qquad (34)$$

2.4.2 Coherence:

The coherence function between the input and the output signals of an e.g., a SDOF system is given by the equation [16]:

$$\widehat{\gamma^2}_{yx}(f_k) = \frac{\left|\hat{P}_{yx}^{PSD}(f_k)\right|^2}{\hat{P}_{xx}^{PSD}(f_k)\hat{P}_{yy}^{PSD}(f_k)} \qquad (35)$$

Where $\widehat{\gamma^2}_{yx}(f_k)$ is an estimate of the Coherence function between input and output signal x(t) respective y(t) and $\hat{P}_{yy}^{PSD}(f_k)$ is an estimate of the powerspectral density for the output signal y(t).

The coherence function between two weakly stationary random signals provides a measure on the linear dependence between the signals as a function of frequency and it assumes values between 0 and 1, i.e. [16]:

- $\hat{C}_{yx}(f_k)$=1 ➔ we do not have any external noise and the measured output y (n) may be explained linearly from the measured input x (n).
- $0<\hat{C}_{yx}(f_k)<1$ ➔ noise may affect the measurements and/or the measured output, y (n), may not be explained linearly from the measured input x(n).
- $\hat{C}_{yx}(f_k) = 0$ ➔ x(n) and y(t) are completely uncorrelated

In table 1 the parameters used for the spectrum estimation are given.

Parameter	Value
Block Length	4096
Window	Hanning
Overlapping	50%
Number of averages	80

Table 1: Parameters used for the spectrum estimation.

2.5 Power Spectral Density Transmissibility (PSDT):

To address power spectral density transmissibility a three-degrees-of-freedom (three DOF) system is considered. In the frequency domain the 3x1 displacement vector $\{X(f)\}$ is related to the 3x1 force vector $\{F(f)\}$ via the 3x3 frequency response function matrix [H(f)] as:

$$\{X(f)\} = [\mathrm{H(f)}]\,\{F(f)\} \tag{36}$$

In the case of a three-degrees-of-freedom system, the frequency response function matrix is given by:

$$[H(f)] = \begin{bmatrix} H_{11}(f) & H_{12}(f) & H_{13}(f) \\ H_{21}(f) & H_{22}(f) & H_{23}(f) \\ H_{31}(f) & H_{32}(f) & H_{33}(f) \end{bmatrix} \tag{37}$$

Where $H_{mn}(f)$ is the frequency response function between the response coordinate m and the force coordinate n, $m, n \in \{1, 2, 3\}$. The frequency response matrix may be expanded as

$$[H(f)] = \sum_{m=1}^{3} \left(\frac{1}{a_m} \frac{\{\Psi\}_m \{\Psi\}_m^T}{j2\pi f - \left(-\omega_m \zeta_m + j\omega_m \sqrt{1-\zeta_m^2}\right)} + \frac{1}{a_m^*} \frac{\{\Psi\}_m^* \{\Psi\}_m^H}{j2\pi f - \left(-\omega_m \zeta_m - j\omega_m \sqrt{1-\zeta_m^2}\right)} \right) \tag{38}$$

Where ω_m is the un-damped angular resonance frequency for mode m, ζ_m is the relative damping coefficient for mode m, a_m is the modal A coefficient for mode m and $\{\Psi\}_m$ is the mode shape vector for mode m, defined as

$$\{\Psi\}_m = \begin{Bmatrix} \Psi_{1m} \\ \Psi_{2m} \\ \Psi_{3m} \end{Bmatrix} \tag{39}$$

Here $\Psi_{jm}, j \in \{1, 2, 3\}$ are the mode shape coefficients for mode m. In terms of unit modal A scaling the frequency response matrix may be expanded as

$$[H(f)] = \sum_{m=1}^{3}\left(\frac{\{\phi\}_m\{\phi\}_m^T}{j2\pi f-\left(-\omega_m\zeta_m+j\omega_m\sqrt{1-\zeta_m^2}\right)}+\frac{\{\phi\}_m^*\{\phi\}_m^H}{j2\pi f-\left(-\omega_m\zeta_m-j\omega_m\sqrt{1-\zeta_m^2}\right)}\right) \quad (40)$$

Where $\{\phi\}_m$ is the normal mode shape vector for mode m, given by:

$$\{\phi\}_m = \begin{Bmatrix}\phi_{1m}\\ \phi_{2m}\\ \phi_{3m}\end{Bmatrix} \quad (41)$$

Here $\phi_{jm}, j \in \{1,2,3\}$ are the mode shape coefficients for normal mode m.

For an at least weakly stationary random process the Power Spectral Density Transmissibility (PSDT) between response coordinates i and j, $i,j \in \{1,2,3\}$, of the three-degrees-of-freedom system with reference to the response coordinate q, $q \in \{1,2,3\}$, is given by [15]:

$$T_{x_i x_j}^{q}(f) = \frac{P_{x_i x_q}(f)}{P_{x_j x_q}(f)} \quad (42)$$

Where $P_{x_i x_q}(\mathrm{f})$ is the cross-power spectral density between the response coordinates i and q, $P_{x_j x_q}(\mathrm{f})$ is the cross-power spectral density between the response coordinates j and q [15]. The cross-power spectral density between the response coordinate i and q may be expanded in terms of frequency response functions between response and the forces exciting the three-degrees-of-freedom system and also the cross-power spectral density between the excitation forces $f_n(t)$ $n \in \{1,2,3\}$, according to[15]:

$$P_{x_i x_q}(\mathrm{f}) = \sum_{r=1}^{N}\sum_{s=1}^{N} H_{is}(f)H_{qr}^{*}(f)P_{f_s f_r}(f) \quad (43)$$

Where $P_{f_s f_r}(f)$ is the cross-power spectral density between excitation forces fs*(t)* and $f_r(t)$, $H_{is}(f)$ is the frequency response function between the response coordinate i and the force coordinate s and $H_{qr}^{*}(f)$ is the frequency response function between the response coordinate q and the force coordinate r and * denotes complex conjugation. The frequency response function between the response coordinate i and the force coordinate s may be expanded according to the modal model as:

$$H_{is}(f) = \sum_{m=1}^{3}\left(\frac{\phi_{im}\phi_{sm}}{j2\pi f-\left(-\omega_m\zeta_m+j\omega_m\sqrt{1-\zeta_m^2}\right)}+\frac{\phi_{im}^{*}\phi_{sm}^{*}}{j2\pi f-\left(-\omega_m\zeta_m-j\omega_m\sqrt{1-\zeta_m^2}\right)}\right) \quad (44)$$

If it is assumed, the eigen modes of the three-degrees-of-freedom system are well separated and that they have low relative damping the frequency response function $H_{is}(f)$, at any of the three damped eigenfrequencies $f_{Dm}, m \in \{1, 2, 3\}$, may be approximated as:

$$H_{is}(f_{Dm}) \approx \frac{\phi_{im}\phi_{sm}}{2\pi f_m\zeta_m} \quad (45)$$

Where $f_m, m \in \{1, 2, 3\}$ is one of the three DOF systems eigenfrequencies. Thus, the cross-power spectral density $P_{x_i\,x_q}(\mathrm{f})$ between the response coordinates i and q at any of the three damped eigenfrequencies $f_{Dm}, m \in \{1, 2, 3\}$, may be approximated as:

$$P_{x_i\,x_q}(f_{Dm}) \approx \sum_{r=1}^{N}\sum_{s=1}^{N}\frac{\phi_{im}\phi_{sm}}{2\pi f_m\zeta_m}\frac{\phi_{qm}^{*}\phi_{rm}^{*}}{2\pi\ m\zeta_m}P_{f_s\,f_r}(f_{Dm}) =$$
$$\phi_{im}\sum_{r=1}^{N}\sum_{s=1}^{N}\frac{\phi_{sm}}{2\pi f_m\zeta_m}\frac{\phi_{qm}^{*}\phi_{rm}^{*}}{2\pi f_m\zeta_m}P_{f_s\,f_r}(f_{Dm}) \quad (46)$$

Furthermore, the cross-power spectral density $P_{x_j\,x_q}(\mathrm{f})$ between the response coordinates j and q at any of the three damped eigenfrequencies $f_{Dm}, m \in \{1, 2, 3\}$, may be approximated as:

$$P_{x_j\,x_q}(f_{Dm}) \approx \sum_{r=1}^{N}\sum_{s=1}^{N}\frac{\phi_{jm}\phi_{sm}}{2\pi f_m\zeta_m}\frac{\phi_{qm}^{*}\phi_{rm}^{*}}{2\pi f_m\zeta_m}P_{f_s\,f_r}(f_{Dm}) =$$
$$\phi_{jm}\sum_{r=1}^{N}\sum_{s=1}^{N}\frac{\phi_{sm}}{2\pi f_m\zeta_m}\frac{\phi_{qm}^{*}\phi_{rm}^{*}}{2\pi f_m\zeta_m}P_{f_s\,f_r}(f_{Dm}) \quad (47)$$

Hence, the Power Spectral Density Transmissibility (PSDT) between response coordinates i and j, $i, j \in \{1, 2, 3\}$, of the three-degrees-of-freedom system with reference to the response coordinate q, $q \in \{1, 2, 3\}$, at any of the three damped eigenfrequencies $f_{Dm}, m \in \{1, 2, 3\}$, is approx. given by [15]:

$$T_{x_i\,x_j}^{q}(f_{Dm}) = \frac{P_{x_i\,x_q}(f_{Dm})}{P_{x_j\,x_q}(f_{Dm})} \approx \frac{\phi_{im}\sum_{r=1}^{N}\sum_{s=1}^{N}\frac{\phi_{sm}}{2\pi f_m\zeta_m}\frac{\phi_{qm}^{*}\phi_{rm}^{*}}{2\pi f_m\zeta_m}P_{f_s\,f_r}(f_{Dm})}{\phi_{jm}\sum_{r=1}^{N}\sum_{s=1}^{N}\frac{\phi_{sm}}{2\pi f_m\zeta_m}\frac{\phi_{qm}^{*}\phi_{rm}^{*}}{2\pi\ m\zeta_m}P_{f_s\,f_r}(f_{Dm})} = \frac{\phi_{im}}{\phi_{jm}} \quad (48)$$

Thus, at any of the damped eigenfrequencies the Power Spectral Density Transmissibility between response coordinates of the system will result in a quotient between the mode shape coefficients for normal mode corresponding to the damped eigenfrequency and that particular response coordinates [15].

2.6 Identification of Modal Parameters using Power Spectral Density Transmissibility

A 3x3 power spectral density transmissibility matrix may be assembled for the three DOF system according to

$$\left[T_{x_{1-3}\,x_j}^{1-3}(f)\right] = \begin{bmatrix} T_{x_1\,x_j}^{1}(f) & T_{x_1\,x_j}^{2}(f) & T_{x_1\,x_j}^{3}(f) \\ T_{x_2\,x_j}^{1}(f) & T_{x_2\,x_j}^{2}(f) & T_{x_2\,x_j}^{3}(f) \\ T_{x_3\,x_j}^{1}(f) & T_{x_3\,x_j}^{2}(f) & T_{x_3\,x_j}^{3}(f) \end{bmatrix} \quad (49)$$

Where $j \in \{1, 2, 3\}$. At any of the three damped eigenfrequencies $f_{Dm}, m \in \{1, 2, 3\}$, power spectral density transmissibility matrix is approx. given by [15]:

$$\left[T_{x_{1-3}\,x_j}^{1-3}(f_{Dm})\right] \approx \begin{bmatrix} \frac{\phi_{1m}}{\phi_{jm}} & \frac{\phi_{1m}}{\phi_{jm}} & \frac{\phi_{1m}}{\phi_{jm}} \\ \frac{\phi_{2m}}{\phi_{jm}} & \frac{\phi_{2m}}{\phi_{jm}} & \frac{\phi_{2m}}{\phi_{jm}} \\ \frac{\phi_{3m}}{\phi_{jm}} & \frac{\phi_{3m}}{\phi_{jm}} & \frac{\phi_{3m}}{\phi_{jm}} \end{bmatrix} \quad (50)$$

This transmissibility matrix has identical columns, the columns are linearly dependent, and thus the matrix has a rank equal to one. Hence, with the aid of the three-power spectral density transmissibility matrices $\left[T_{x_{1-3}\,x_j}^{1-3}(f_{Dm})\right]$, $j \in \{1, 2, 3\}$, in combination with singular value decomposition (SVD) the three damped eigenfrequencies $f_{Dm}, m \in \{1, 2, 3\}$, of the three DOF system may be estimated [15]. The power spectral density transmissibility matrix $\left[T_{x_{1-3}\,x_j}^{1-3}(f_{Dm})\right]$ may be decomposed with the aid of the SVD according to [15]:

$$\left[T_{x_{1-3}\,x_j}^{1-3}(f)\right] = \left[U_j(f)\right]\left[\Sigma_j(f)\right]\left[V_j(f)\right]^H \quad (51)$$

Where $[\bullet]^H$ denotes Hermitian transpose, $\left[U_j(f)\right]$ is a 3x3 matrix and $\left[V_j(f)\right]$ is a 3x3 matrix. Both and are unitary

matrices, i.e. $\left[U_j(f)\right]\left[U_j(f)\right]^H = [I]$, $\left[V_j(f)\right]\left[V_j(f)\right]^H = [I]$, (Columns and rows are orthonormal). Furthermore, $\left[\Sigma_j(f)\right]$ is a diagonal matrix according to:

$$\left[\Sigma_j(f)\right] = \begin{bmatrix} \sigma_{1j}(f) & 0 & 0 \\ 0 & \sigma_{2j}(f) & 0 \\ 0 & 0 & \sigma_{3j}(f) \end{bmatrix} \qquad (52)$$

Where $\sigma_{1j}(f) \geq \sigma_{2j}(f) \geq \sigma_{3j}(f)$ are the singular values of the power spectral density transmissibility matrix $\left[T^{1-3}_{x_{1-3}\,x_j}(f_{Dm})\right]$ and they are real and positive numbers [15]. Since the power spectral density transmissibility matrix has a rank equal to one at any of the three damped eigenfrequencies $f_{Dm}, m \in \{1, 2, 3\}$, it yields that

$$\sigma_{2j}(f_{Dm}) = \sigma_{3j}(f_{Dm}) = 0,\ j \in \{1, 2, 3\}$$

The damped eigenfrequencies and the mode shapes of an operating structure may be estimated with the aid of the singular value decomposition of the power spectral density transmissibility matrices with different references, the so-called PSDTM-SVD method [15]. Basically, if the response of an operating structure has been measured at M spatial position of the structure the power spectral density transmissibility matrices $\left[T^{1-M}_{x_{1-M}\,x_j}(f)\right]$, $j \in \{1, 2, \ldots, \mathrm{M}\}$, are estimated. Subsequently the singular values, $\sigma_{1j}(f), \sigma_{2j}(f), \ldots, \sigma_{Mj}(f)$, for these matrices are calculated. Based on these singular-values the invers of each of the singular-values except for $\sigma_{1j}(f)$ are assembled in vectors according to:

$$\Sigma_j^{-1}(f) = \left\{\frac{1}{\sigma_{2j}(f)} \ \frac{1}{\sigma_{3j}(f)} \cdots \frac{1}{\sigma_{Mj}(f)}\right\} \qquad (53)$$

Based on these vectors their arithmetic mean value is calculated as

$$\hat{\Sigma}^{-1}(f) = \frac{1}{M}\sum_{j=1}^{M}\left\{\frac{1}{\sigma_{2j}(f)} \ \frac{1}{\sigma_{3j}(f)} \cdots \frac{1}{\sigma_{Mj}(f)}\right\} = \left\{\frac{1}{\hat{\sigma}_2(f)} \ \frac{1}{\hat{\sigma}_3(f)} \cdots \frac{1}{\hat{\sigma}_M(f)}\right\} \qquad (54)$$

In the so-called PSDTM-SVD method a function for the estimation of the damped eigenfrequencies f_{Dm} of an operating structure is defined as [15]:

$$\pi(f) = \prod_{m=2}^{M} \frac{1}{\widehat{\sigma}_m(f)} \qquad (55)$$

The frequency values of the peaks in the spectrum of the function π(f) provides the estimates of the damped eigenfrequencies f_{Dm} [15]. Based on the estimates of the damped eigenfrequencies f_{Dm} the corresponding mode shapes may be estimated as [15]:

$$\left\{\widehat{U}(f)\right\}_1 = \frac{1}{M}\sum_{j=1}^{M}\left\{U_j(f)\right\}_1 (56)$$

Where $\left\{U_j(f)\right\}_1$ is the first singular column vector in the left singular vector matrix [15]:

$$\left\{\widehat{U}(f_{Dm})\right\}_1 = \frac{1}{M}\sum_{j=1}^{M}\left\{U_j(f_{Dm})\right\}_1 \qquad (57)$$

Where $\left\{U_j(f_{Dm})\right\}_1$ is the first column vector in the left orthonormal matrix of the SVD of the power spectral density transmissibility matrix $\left[T_{x_{1-3}\,x_j}^{1-3}(f_{Dm})\right]$ at the damped eigenfrequencies f_{Dm} and the left orthonormal matrix is given by [15]:

$$\left[U_j(f_{Dm})\right] = \left[\left\{U_j(f_{Dm})\right\}_1 \left\{U_j(f_{Dm})\right\}_2 \cdots \left\{U_j(f_{Dm})\right\}_M\right] \quad (58)$$

3. Result:

3.1 Time records of jaw crusher acceleration responses

Four different measurements of the acceleration response of a jaw crusher have been carried out. In each measurement, the two triaxial accelerometers were attached to two of three predefined positions on the jaw crusher. The three predefined positions on the jaw crusher are crusher foot (CRF), sidewall of the crusher (SW) and substructure (SS). Moreover, each of the accelerometers measure vibration in three orthogonal directions; the x-direction, the acceleration in the crusher's longitudinal direction, the y-direction, the acceleration in the crusher's vertical direction, and the z-direction, the acceleration in the crusher's transverse/lateral direction. In Fig. 9 the acceleration response at the crusher foot (CRF) position in the x, y and z directions are shown.

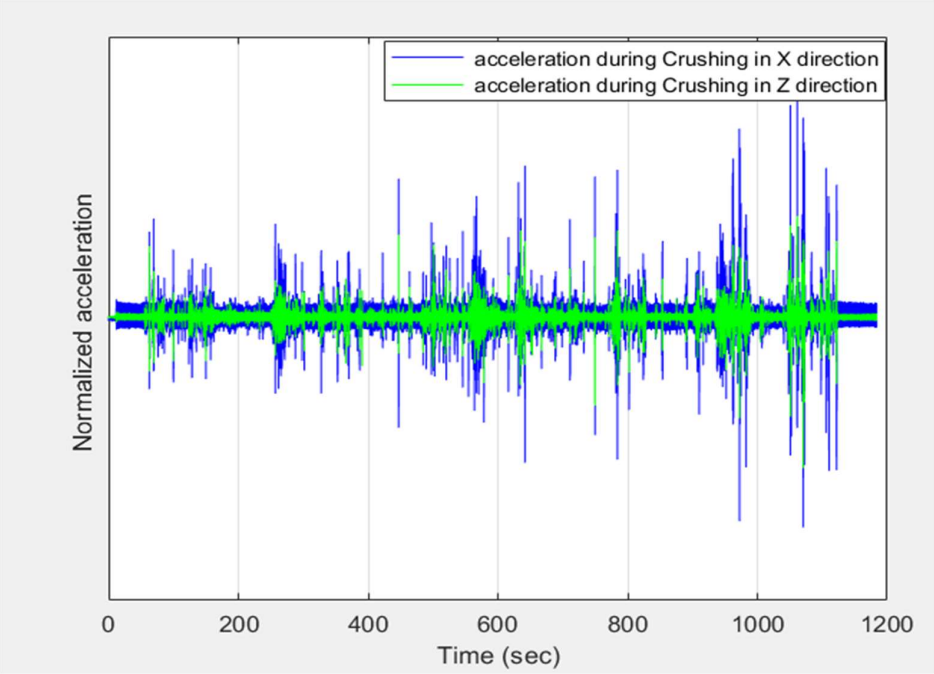

Figure 7: Acceleration response at the crusher foot (CRF) position in the x and z directions.

The acceleration responses at the sidewall (SW) position in the x and z directions are shown in Fig. 8.

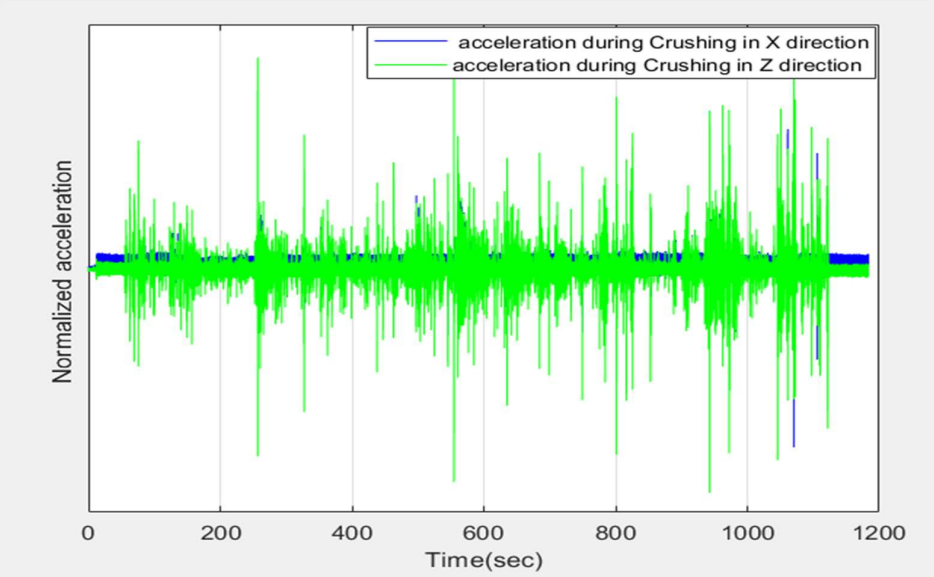

Figure 8: Acceleration response at the sidewall (SW) position in the x and z directions.

Correspondingly, in Fig. 9 the acceleration response at the substructure (SS) position in the x and z directions are shown.

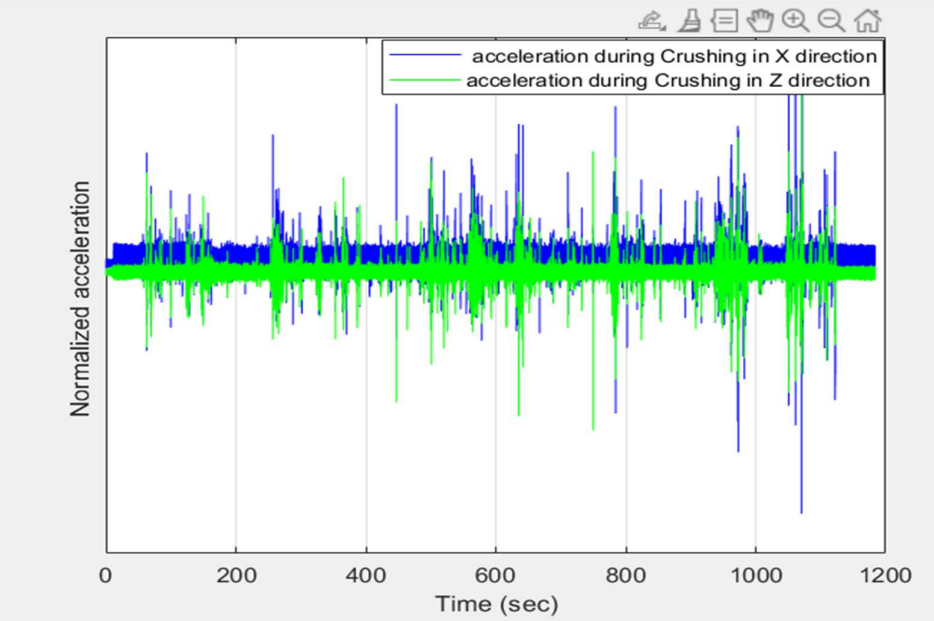

Figure 9: Acceleration response at the substructure (SS) position in the x and z directions.

3.1.1 Modified Time records of jaw crusher acceleration responses.

The measurement of the acceleration responses of the jaw crusher were carried out over time intervals that include both stone crushing and idling without any stone crushing. To only consider acceleration data excited by stone crushing; the time segments of the acceleration records corresponding to idling operation of the jaw cruncher were removed from the acceleration records. Vibration excreted by the periodic motion of the jaws, etc. was also removed in the time records with the aid of a 4 Hz notch filter. In this way, modified time records of jaw crusher acceleration responses were produced.

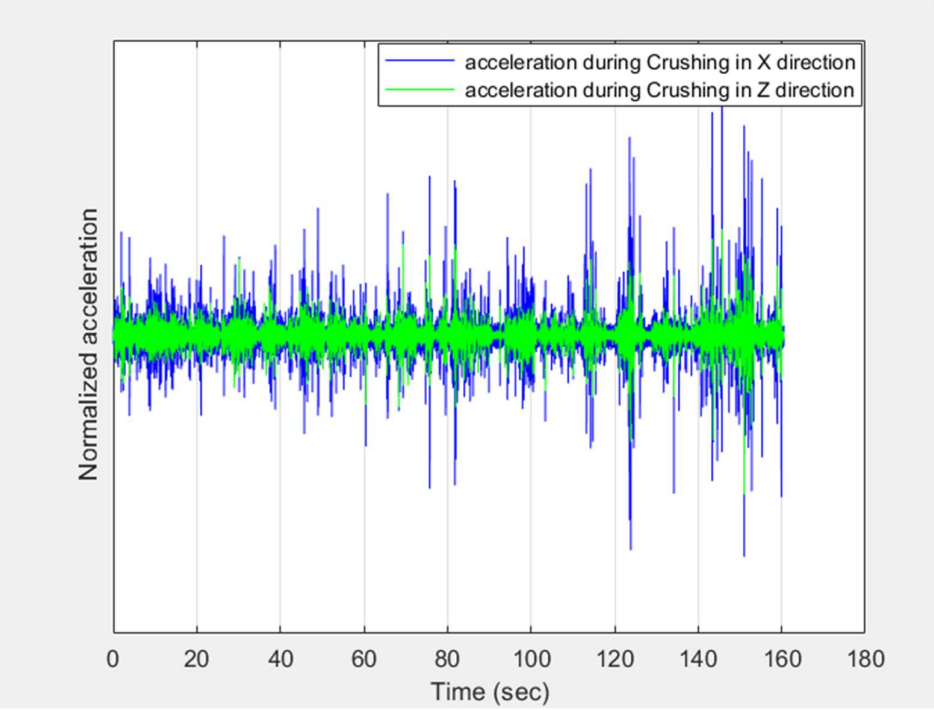

Figure 10: Acceleration response at the crusher foot (CRF) position in the x and z directions without idling.

The acceleration responses at the sidewall (SW) position in the x and z directions without idling are shown in Fig. 11.

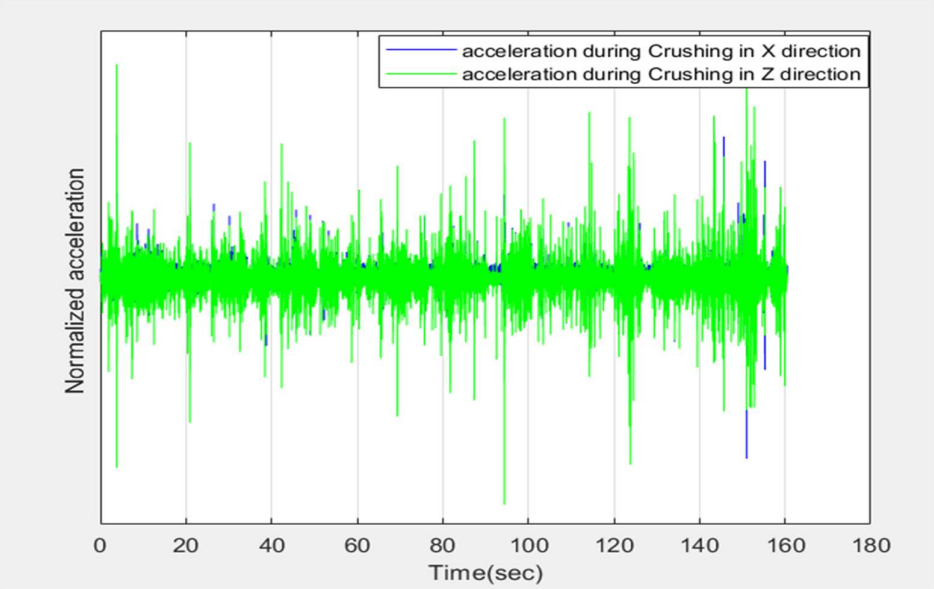

Figure 11: Acceleration response at the sidewall (SW) position in the x and z directions without idling.

Correspondingly, in Fig. 12 the acceleration response at the substructure (SS) position in the x and z directions without idling are shown.

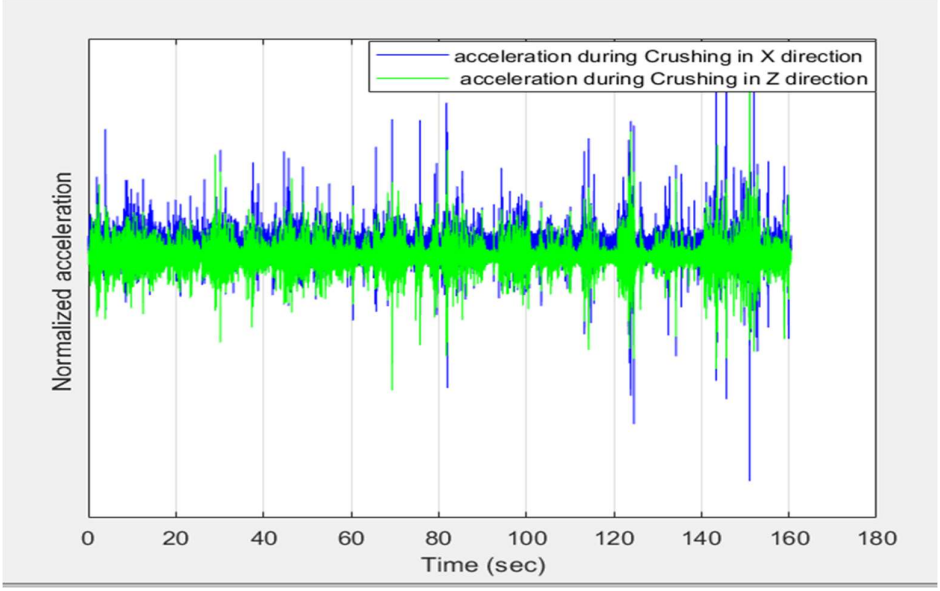

Figure 12: Acceleration response at the substructure (SS) position in the x and z directions without idling.

3.2 Transmissibility and coherence function estimates

Transmissibility functions were estimate for each of the x-, y- and z-directions as well as between the x-, y- and z-directions for the measured acceleration responses of the jaw crusher at the crusher foot (CRF), sidewall (SW) and substructure (SS). Both transmissibility estimates and corresponding coherence functions were estimated using the modified time records of jaw crusher acceleration responses. In the modified time records of jaw crusher acceleration, the time segments of the acceleration records corresponding to idling operation of the jaw crusher were removed from the acceleration records. In fig. 13 the transmissibility function estimate between the acceleration of the crusher foot and the crusher sidewall in the x-direction is shown. The corresponding coherence function estimate between the acceleration of the crusher foot and the crusher sidewall in the x-direction is shown in Fig. 14.

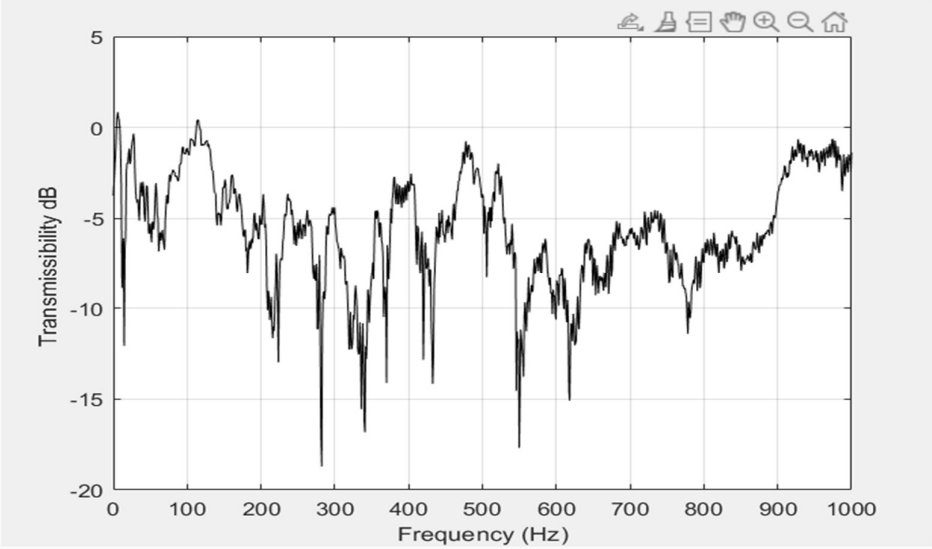

Figure 13: Transmissibility function estimate between the acceleration of the crusher foot and the crusher sidewall in the x-direction without idling.

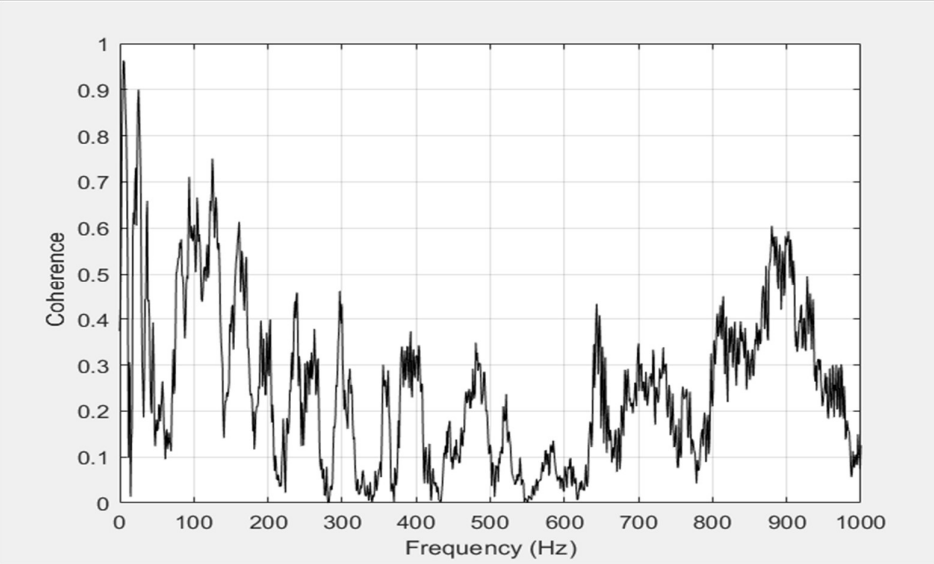

Figure 14: Coherence function estimate between the acceleration of the crusher foot and the crusher sidewall in the x-direction without idling.

In fig. 15 the transmissibility function estimate between the acceleration of the crusher foot and the crusher sidewall in the y-direction is shown. The corresponding coherence function estimate between the acceleration of the crusher foot and the crusher sidewall in the y-direction is shown in Fig. 16.

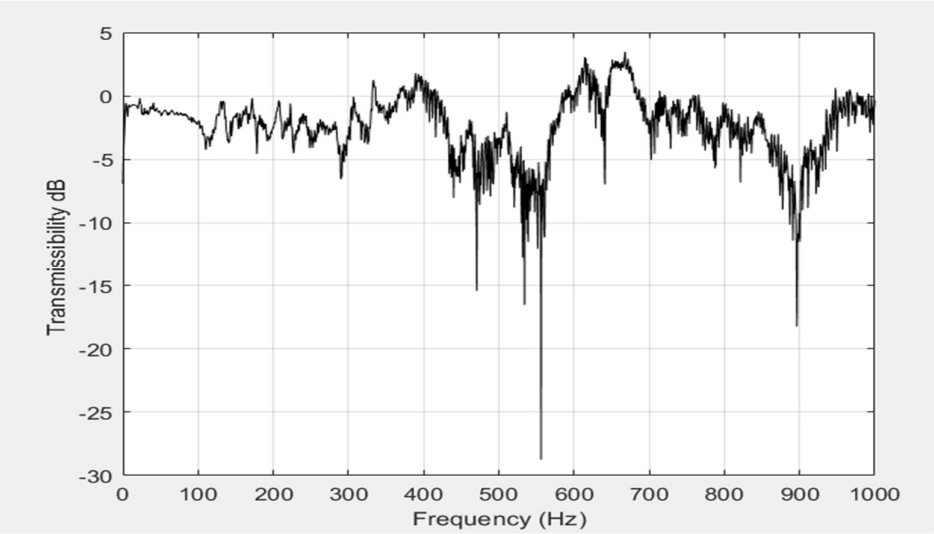

Figure 15: Transmissibility function estimate between the acceleration of the crusher foot and the crusher sidewall in the y-direction without idling.

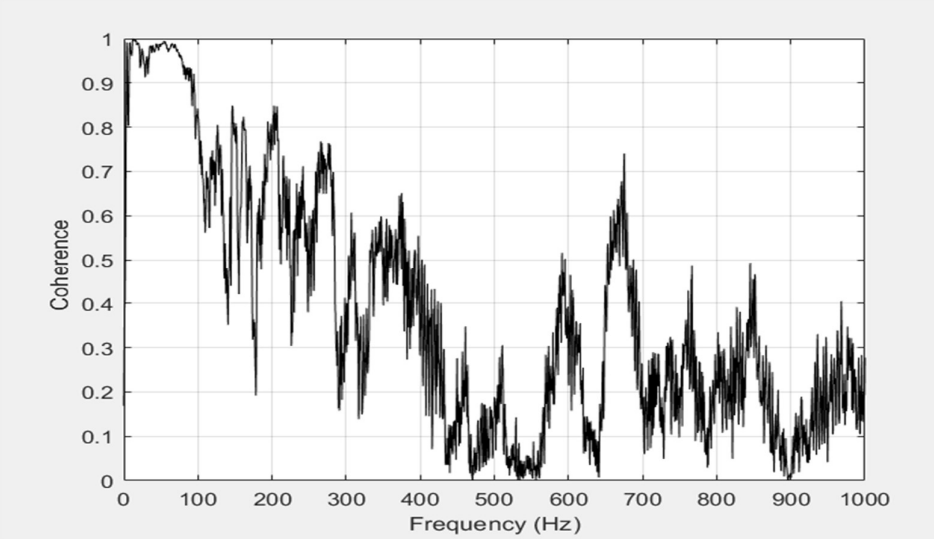

Figure 16: Coherence function estimate between the acceleration of the crusher foot and the crusher sidewall in the y-direction without idling.

In fig. 17 the transmissibility function estimate between the acceleration of the crusher foot and the crusher substructure in the y-direction is shown. The corresponding coherence function estimate between the acceleration of the crusher foot and the crusher substructure in the y-direction is shown in Fig. 18.

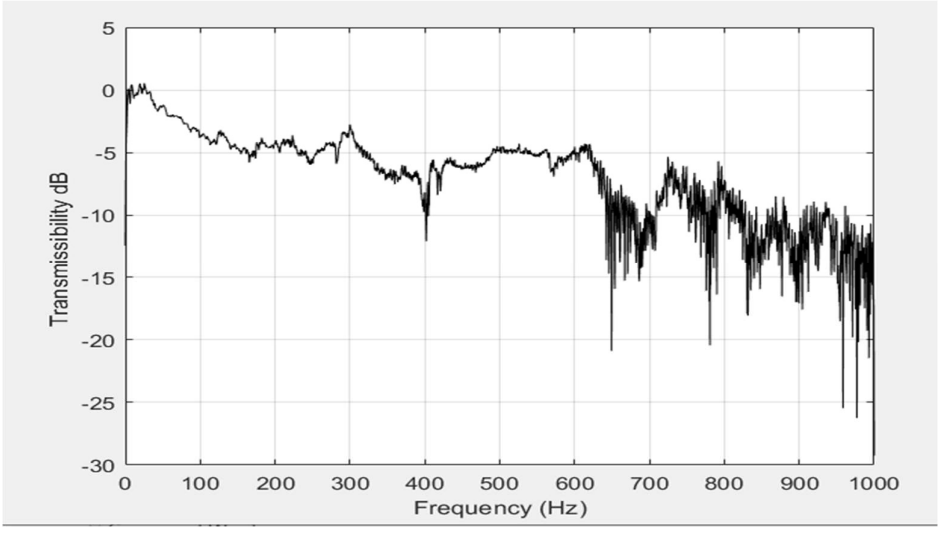

Figure 17: Transmissibility function estimate between the acceleration of the crusher foot and the crusher substructure in the y-direction without idling.

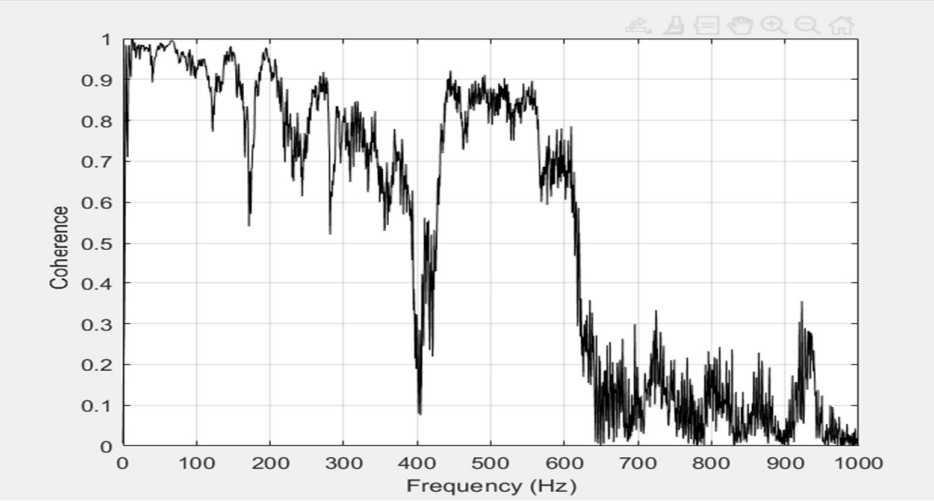

Figure 18: Coherence function estimate between the acceleration of the crusher foot and the crusher substructure in the y-direction without idling.

In fig. 19 the transmissibility function estimate between the acceleration of the crusher sidewall and the crusher substructure in the y-direction is shown. The corresponding coherence function estimate between the acceleration of the crusher sidewall and the crusher substructure in the y-direction is shown in Fig. 20.

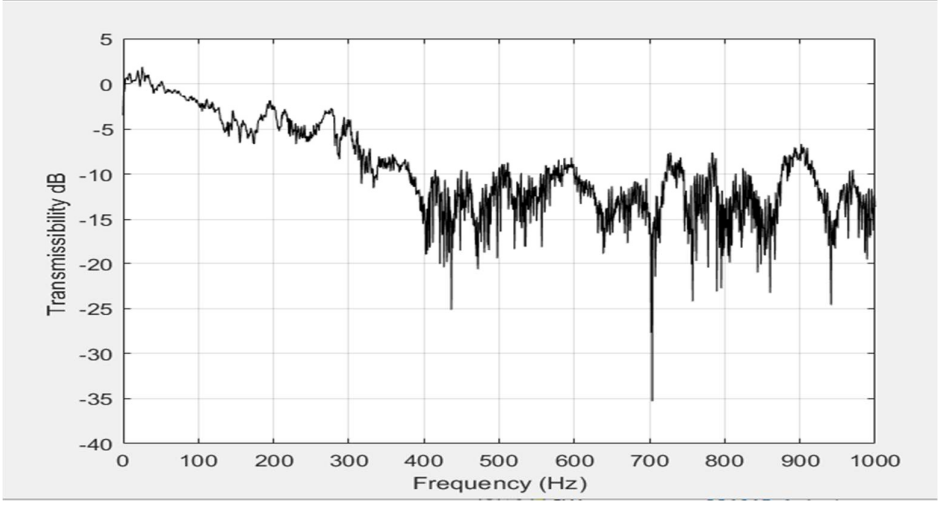

Figure 19: Transmissibility function estimate between the acceleration of the crusher sidewall and the crusher substructure in the y-direction without idling.

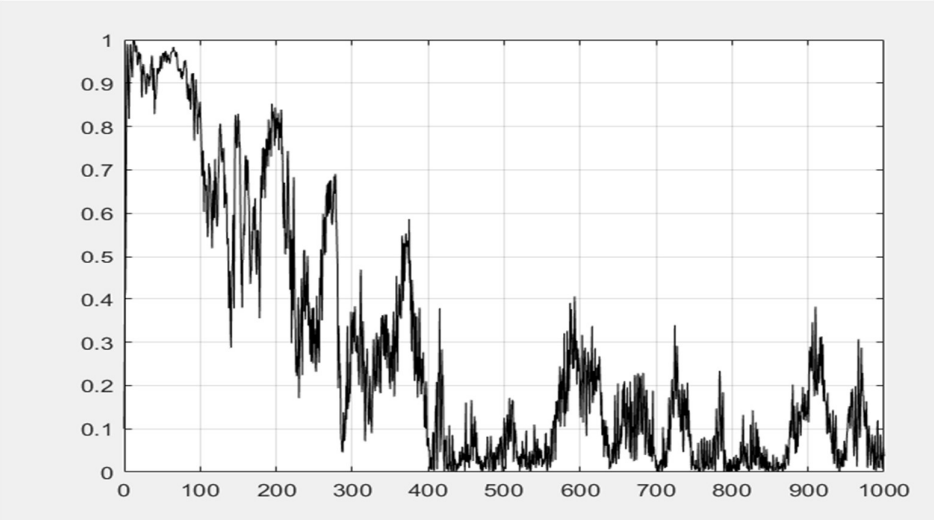

Figure 20: Coherence function estimate between the acceleration of the crusher sidewall and the crusher substructure in the y-direction without idling.

3.3 Estimation of damped natural frequencies of the jaw cruncher.

To estimate damped eigenfrequencies of the jaw crusher during operation the the so-called PSDTM-SVD method [15] was utilized. Based on the modified time records of jaw crusher acceleration responses a number of $\pi(f)$ functions were estimated.

In fig. 21 the PSDTM-SVD methods $\pi(f)$ function for the measured acceleration responses of the jaw crusher in the x-direction is shown

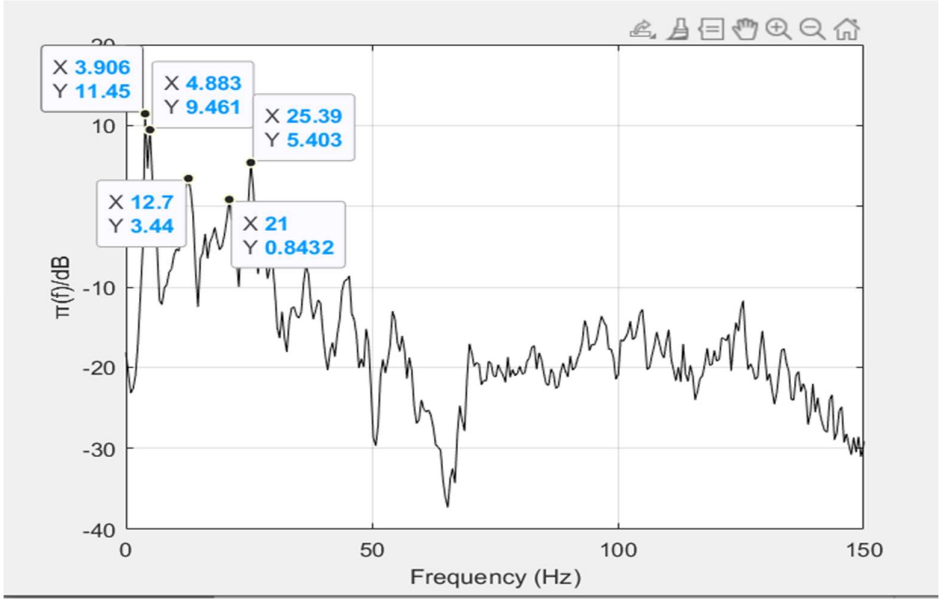

Figure 21: The PSDTM-SVD methods π(f) function for the measured acceleration responses of the jaw crusher in the x-direction. 4 HZ notch filter.

Fig. 22 shows the PSDTM-SVD methods π(f) function for the measured acceleration responses of the jaw crusher in the y-direction.

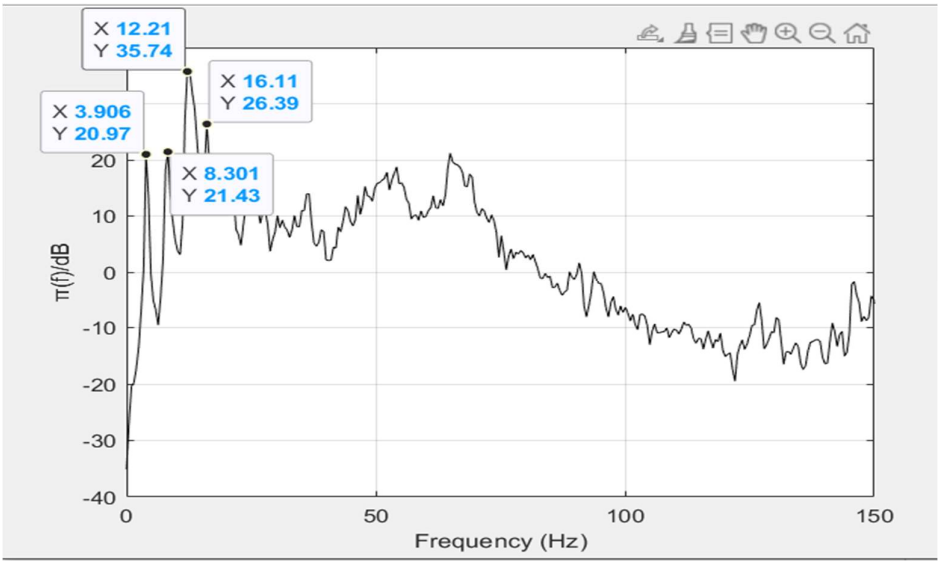

Figure 22: The PSDTM-SVD methods π(f) function for the measured acceleration responses of the jaw crusher in the y-direction. 4 HZ notch filter.

For the z-direction the PSDTM-SVD methods π(f) function for the measured acceleration responses of the jaw crusher is shown in Fig. 23.

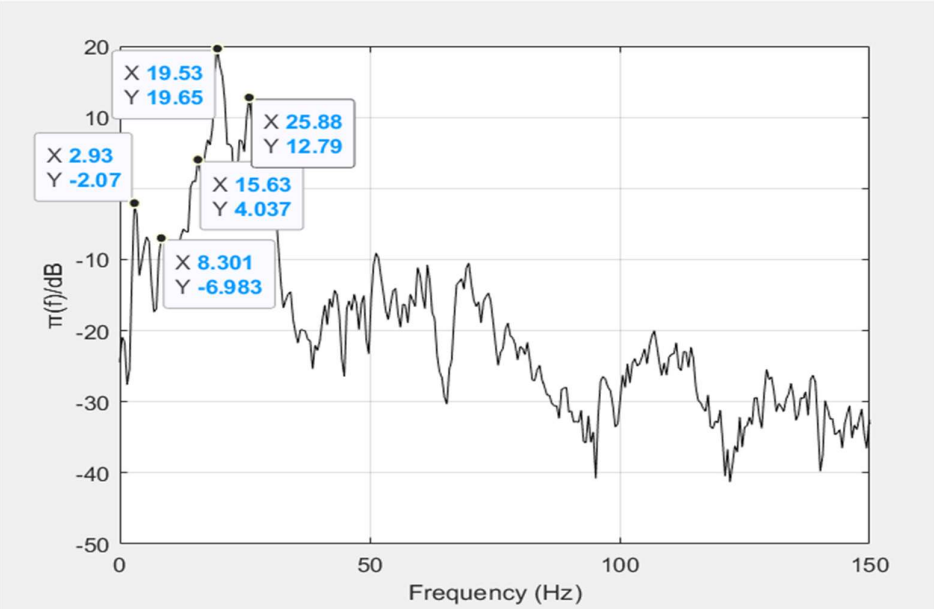

Figure 23: The PSDTM-SVD methods π(f) function for the measured acceleration responses of the jaw crusher in the z-direction. 4 HZ notch filter.

Finally, in Fig. 24 the PSDTM-SVD methods π(f) function for the measured acceleration responses of the jaw crusher in the x-, y- and z-directions is shown.

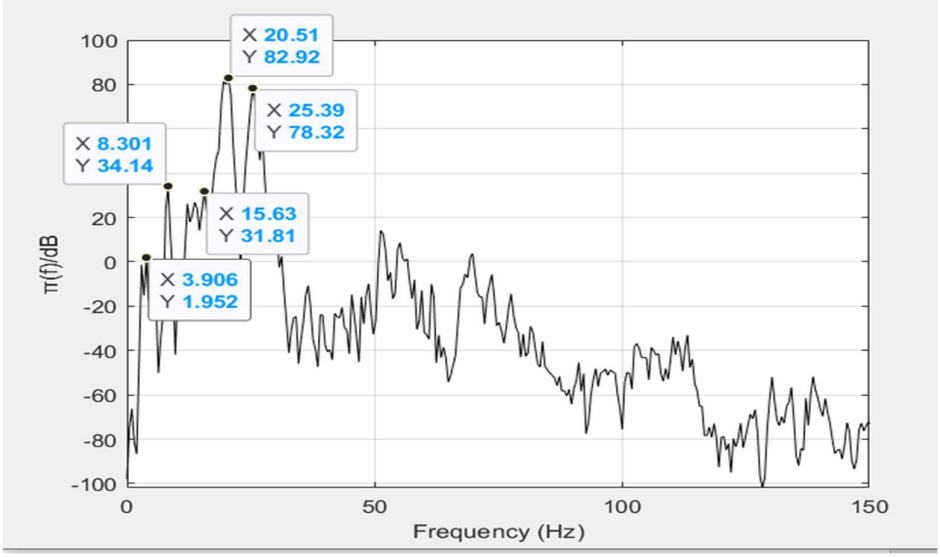

Figure 24: The PSDTM-SVD methods π(f) function for the measured acceleration responses of the jaw crusher in the x-, y- and z-directions. 4 HZ notch filter.

The frequency values of the peaks in the spectrum of the functions π(f) in Figs. 21 - 24 provides estimates of the damped eigenfrequencies f_{Dm} of the jaw crusher. In table 2 the frequencies of pronounced peaks in the spectrum of the functions π(f) in Figs. 21 – 24 are given.

X-direction [Hz]	Y-direction [Hz]	Z-direction [Hz]	X-,Y- and Z-directions [Hz]
3.9	3.9	2.9	3.9
4.8	8.3	8.3	8.3
12.7	12.7	15.3	15.6
21	16.1	19.3	20.5
25.4	25.39	25.8	25.4

Table 2: Frequency values of pronounced peaks in the spectrum of the functions π(f) in Figs. 21 – 24.

Observe that the notch filter is cantered at 4 Hz and there is peaks at 2.9 Hz, at 3.9 Hz and at 4.8 Hz in the π(f) functions.

4. Summery and Conclusion

To further, improve the design of sub-structures for jaw crusher installations it is imperative to further increase the knowledge concerning the loads applied by the jaw crusher to the substructure during operation. Such knowledge may be acquired with the aid of estimates of acceleration transmissibility functions between the sub-structure and the jaw crusher in a jaw crusher installation during operation. Displacement transmissibility and force transmissibility for MDOF systems have been addressed in section 2.2.2. Based on equations in this section force transmissibility may be derived based on acceleration transmissibility for e.g., MDOF systems. Thus, by assuming certain force lodes on the jaw crusher structure the force load on its sub-structure may be estimated. Transmissibility functions were estimate for each of the x-, y- and z-directions as well as between the x-, y- and z-directions for the measured acceleration responses of the jaw crusher at the crusher foot (CRF), sidewall (SW) and substructure (SS). However, only for the y-direction, in the frequency range up to approx. 100 Hz, a coherence of approx. 0.9 and higher were obtained (see Figs. 16-20).

To estimate damped eigenfrequencies of the jaw crusher during operation the so-called PSDTM-SVD method [15] was utilized. Based on the modified time records of jaw crusher acceleration responses a number of $\pi(f)$ functions were estimated. The jaw crusher acceleration responses in the modified time records are attenuated at 4 Hz. Thus, peaks in the $\pi(f)$ function in the range of 4 Hz are not likely to be reliable as estimates of the damped eigenfrequencies jaw crusher. Table 2 suggests that 8, 13, 16, 20 and 25 Hz may be considered as estimates of damped eigenfrequencies of the operating jaw crusher.

5. Reference

1. https://en.wikipedia.org/wiki/Crusher#cite_note-1

2. The following link gives a good overview of the crusher motion: https://www.youtube.com/watch?v=JEXbX2SYvBM.

3. https://www.youtube.com/watch?v=EE5J6prm1y8

4. http://www.tlt.as/Undersider/documents/JawCrusher.pdf

5. Cao, J., X. Rong and S. Yang (2006). Jaw Plate Kinematical Analysis for Single Toggle Jaw Crusher Design. *International Technology and Innovation Conference, 2006, Section 1: Advanced Manufacturing Technology. Pages 62-66*.

6. http://www.rockproducts.com/index.php/features/51-archives/1240.pdf

7. Zhong, L. and K. Chen (2010). Study on Digital Platform for Jaw Crusher Design. *2010 International Conference on Mechanics Automation and Control Engineering*. IEEE.

8. Mular, A. L., N. H. Doug and D. J. Barrat (2002). *Mineral Processing Plant Design, Practice and Control*: *Proceedings, Volume 1, pages 584 to 605*.Society for Mining, Metallurgy and Exploration, Incorporated (SME).

9. https://community.sw.siemens.com/s/article/window-types-hanning-flattop-uniform-tukey-and-exponential

10. Lars Håkansson, S 2016, Diagnos på distans – online engineering på masternivå, Lecture notes, Diagnos 1 ET2608, Linnaeus University, Delivered 6 February 2019.

11. S. Chilakapati, September 2016, Study of vibration Transmissibility of Operational Industrial Machines (Master's Thesis), Blekinge Tekniska Högskola (BTH), Karlskrona, Sweden.

12. L. Håkansson, S 2016, Diagnos på distans – online engineering på masternivå, Lecture notes, Modellering 2 ET1514, Linnaeus University, Delivered 6 February 2019

13. Y.E. Lage, M.M. Neves, N.M.M. Maia and D. Tcherniak, Force transmissibility versus displacement transmissibility, Journal of Sound and Vibration, Vol. 333, pp. 5708 - 5722, 2014; http://dx.doi.org/10.1016/j.jsv.2014.05.038i

14. Sandvik AB company

15. I. G. Araújo and J. E. Laier, Operational modal analysis using SVD of power spectral density transmissibility matrices, Department of Structural Engineering, University of São,Av. Trabalhador Saocarlense, 400, CEP 13566-590 São Carlos, Brazil , journal homepage: www.elsevier.com/locate/ymssp.

16. A. Brandt, Noise and Vibration Analysis: Signal Analysis and Experimental Procedures, John Wiley & Sons, Inc, 2011.

17. P.D. Welch, "The Use of Fast Fourier Transform for the Estimation of Power Spectra: A Method Based on Time Averaging Over Short, Modified Periodograms", IEEE Transactions on Audio and Electroacoustics, June 1967.

6. Appendix

6.1 MATLAB Code:

```
% Sandvik Data:

Clc ;

close all;

% Each data is consisting of 3 acceleration measurements at 3 position on the
% jaw crusher which are: -CRF (Crusher foot); - SW (Side wall of the
% crusher); - SS (substructure), moreover; Each one of this position has
% acceleration data in 3 direction X(Longitudinal), Y(Vertical), Z
% (Transverse/lateral).

load ('Acc_test_session1_test1.mat', 'data_acc')

SW_1 =data_acc(1,1);
CRF_1=data_acc(2,1);
SS_1=data_acc(3,1);

%for CRF (Crusher Foot):

% data in x direction

 CRF_x= CRF_1.x([135000:141000 512000:546000 653000:664000
993000:1008000 1031000:1041000 1090000:1098000 1120000:1166000
1262000:1284000 1557000:1574000 1646000:1656000 1876000:1976000
2094000:2105000 2121000:2129000 2137000:2148000 2210000:2222000]);

% data in y direction

 CRF_y= CRF_1.y([135000:141000 512000:546000 653000:664000
993000:1008000 1031000:1041000 1090000:1098000 1120000:1166000
1262000:1284000 1557000:1574000 1646000:1656000 1876000:1976000
2094000:2105000 2121000:2129000 2137000:2148000 2210000:2222000]);
```

```
% data in z direction

 CRF_z= CRF_1.z([135000:141000 512000:546000 653000:664000
993000:1008000 1031000:1041000 1090000:1098000 1120000:1166000
1262000:1284000 1557000:1574000 1646000:1656000 1876000:1976000
2094000:2105000 2121000:2129000 2137000:2148000 2210000:2222000]);

 %for SW (Side wall of the Crusher):

% data in x direction

  SW_x= SW_1.x([135000:141000 512000:546000 653000:664000
993000:1008000 1031000:1041000 1090000:1098000 1120000:1166000
1262000:1284000 1557000:1574000 1646000:1656000 1876000:1976000
2094000:2105000 2121000:2129000 2137000:2148000 2210000:2222000]);

% data in y direction

  SW_y= SW_1.y([135000:141000 512000:546000 653000:664000
993000:1008000 1031000:1041000 1090000:1098000 1120000:1166000
1262000:1284000 1557000:1574000 1646000:1656000 1876000:1976000
2094000:2105000 2121000:2129000 2137000:2148000 2210000:2222000]);

% data in z direction

  SW_z= SW_1.z([135000:141000 512000:546000 653000:664000
993000:1008000 1031000:1041000 1090000:1098000 1120000:1166000
1262000:1284000 1557000:1574000 1646000:1656000 1876000:1976000
2094000:2105000 2121000:2129000 2137000:2148000 2210000:2222000]);

%for SS (Substructure):

% data in x direction

 SS_x= SS_1.x([135000:141000 512000:546000 653000:664000
993000:1008000 1031000:1041000 1090000:1098000 1120000:1166000
1262000:1284000 1557000:1574000 1646000:1656000 1876000:1976000
2094000:2105000 2121000:2129000 2137000:2148000 2210000:2222000]);
```

```
% data in y direction

SS_y= SS_1.y([135000:141000 512000:546000 653000:664000
993000:1008000 1031000:1041000 1090000:1098000 1120000:1166000
1262000:1284000 1557000:1574000 1646000:1656000 1876000:1976000
2094000:2105000 2121000:2129000 2137000:2148000 2210000:2222000]);

% data in z direction

 SS_z= SS_1.z([135000:141000 512000:546000 653000:664000
993000:1008000 1031000:1041000 1090000:1098000 1120000:1166000
1262000:1284000 1557000:1574000 1646000:1656000 1876000:1976000
2094000:2105000 2121000:2129000 2137000:2148000 2210000:2222000]);


 % Given:
  N =length (SS_x); % length of the signal
  fs =2000;    % sample frequency
  Ts =1/fs;    % sample time
  T =0: Ts:Ts*(N-1);  %Time of signal




%test 3x3 Matrix data:

% remove the mean value from the data

x_1(:,1)=CRF_y;
x_1(:,2)=SW_y;
x_1(:,3)=SS_y;

X_mean1 =mean(x_1(:,1));
X_mean2 =mean(x_1(:,2));
X_mean3 =mean(x_1(:,3));

x_2(:,1)=x_1(:,1)-X_mean1;
x_2(:,2)=x_1(:,2)-X_mean2;
x_2(:,3)=x_1(:,3)-X_mean3;
```

```
%filtering data:

w0= 4/(2000/2);
  BW = w0/1;
  [b,a] = iirnotch(w0,BW);

  y_1 = filter(b,a,x_2(:,1));
  y_2 = filter(b,a,x_2(:,2)) ;
  y_3 = filter(b,a,x_2(:,3));


  % result data
x_3(:,1)=y_1;
x_3(:,2)=y_2;
x_3(:,3)=y_3;

f=(0:2048)'*fs/4096;


  % PSDT and SVD matrix (Power Spectral Density Transmissibility Matrix
) and (Singular Value Decompostion):

for in=1:3
   for out =1:3

Gxx(:,out,in)=squeeze(cpsd(x_3(:,in),x_3(:,out),hanning(4096),0,4096,fs))/fs
*2 ;
   end
end


sv=zeros(2049,3,3);
for si=1:2049
   [U,S,V] = svd(squeeze(Gxx(si,:,:)));
sv(si,:,:)=S;
end
figure
hold
for n=1:3
   plot(f,10*log10(sv(:,n,n)))
end
xlim([0 150])
grid on
title('Cpsd vs Frequency')
```

```
xlabel('Frequency (Hz)')
ylabel('Cross Power spectral density (SVD)')

%%%%%%%%%%%%%%%%%%

for j=1:3
T3tot(:,1,:)=[squeeze(Gxx(:,1,1))./squeeze(Gxx(:,j,1))
squeeze(Gxx(:,2,1))./squeeze(Gxx(:,j,1))
squeeze(Gxx(:,3,1))./squeeze(Gxx(:,j,1)) ];
T3tot(:,2,:)=[squeeze(Gxx(:,1,2))./squeeze(Gxx(:,j,2))
squeeze(Gxx(:,2,2))./squeeze(Gxx(:,j,2))
squeeze(Gxx(:,3,2))./squeeze(Gxx(:,j,2)) ];
T3tot(:,3,:)=[squeeze(Gxx(:,1,3))./squeeze(Gxx(:,j,3))
squeeze(Gxx(:,2,3))./squeeze(Gxx(:,j,3))
squeeze(Gxx(:,3,3))./squeeze(Gxx(:,j,3)) ];

sv3tot=zeros(1000,3,3);
sumsing=zeros(1000,3);
remove=zeros(1000,3);
invsvav=zeros(1000,3);
pinvsvav=zeros(1000,3);
for si3tot=1:1000
   [U3tot,S3tot,V3tot] = svd(squeeze(T3tot(si3tot,:,:)));
sv3tot(si3tot,:,:)=S3tot;
end
for l=1:3
sumsing(:,l)=sumsing(:,l)+1./sv3tot(:,l,l);

if j==1
   remove(:,l)=1./sv3tot(:,l,l);
end
end
end
invsvav=1/5*(sumsing-remove);
pinvsvav=prod(invsvav,[2]);
figure;plot(f(1:1000),10*log10(pinvsvav))
xlim([0 150])
grid on
 title('SVD vs Frequency')
 xlabel('Frequency (Hz)')
 ylabel('SVD inverse S(2,2)')
  legend('inverse S(2,2)')
```